Bulg. J. Phys. **43** (2016) 110–120

The Effect of Process Parameters in Femtosecond Laser Micromachining*

K. Garasz[1], **M. Tański**[1], **M. Kocik**[1], **E. Iordanova**[2], **G. Yankov**[2], **S. Karatodorov**[2], **M. Grozeva**[2]

[1]Centre for Plasma and Laser Engineering, The Szewalski Institute of Fluid Flow Machinery, Polish Academy of Sciences. Fiszera 14, 80-231 Gdańsk, Poland

[2]Laboratory of Metal Vapour Lasers, Georgi Nadjakov Institute of Solid State Physics, Bulgarian Academy of Sciences, 72 Tzarigradsko Chaussee Blvd., 1784 Sofia, Bulgaria

Received *17 May 2016*

Abstract. The paper presents extensive parametric study on ultrashort pulse laser micromachining of different materials. The experiment was conducted using SpectraPhysics femtosecond laser system. The laser offers 35 fs pulses with tunable wavelength and 1 kHz repetition rate. Therefore, the system itself allows to perform a complex research for a wide range of various parameters and materials.

Laser micromachining is a process based on a laser ablation phenomenon, i.e. microscopic removal of the material from the sample surface during laser irradiation. The process is strongly dependent from the applied laser radiation parameters and is considered the most precise method of material removal. The use of femtosecond laser pulses in micromachining allows a high concentration of energy within a single laser pulse and enables the detachment of particles from the irradiated target without any thermal damage to the surrounding material. The removal of the material occurs in the Rayleigh range from the laser focus.

The effect of laser fluence, wavelength, and machining process velocity on the crater size was measured and analyzed. It has been established, that the quality and efficiency of laser ablation process using femtosecond pulses allows to avoid most of the unwanted effects of the heat affected zone. The use of ultrashort laser pulses creates therefore an attractive opportunity for precise micromachining of many groups of materials.

PACS codes: 79.20.Eb

*This paper has been presented at the International Workshop on Laser and Plasma Matter Interaction, 18-20 November, 2015, Plovdiv, Bulgaria

1 Introduction

The research problem presented in this paper is a parametric study of the short-pulsed laser interactions with matter during micromachining process. Although the research topic itself is very popular in the scientific community, it is relatively little elucidated and lacks a complex approach. The experimental results obtained from the study and further theoretical considerations will allow to verify the existing theories on laser-matter interactions and increase the applicability of short-pulse laser micromachining. The experimental investigations were carried out on different materials (metals and plastics), which are considered industrially relevant.

Micromilling and drilling, surface structuring, cutting and scribing have been used on both, metals and dielectrics to create micromechanical devices (MEMS, MOEMS), nozzles, solder masks and stencils, biomedical device, micro-optics (micro-lenses, diffractive elements), photonics devices (optical waveguides, telecommunications devices) and more [1].

The investigation of the post-processing craters in the material samples is important for demonstrating the effect of a various laser parameters on micromachining process. The further analysis and interpretation of the results leads to understanding the laser ablation phenomena, which occurs during a highly energetic laser irradiation of the material, and results in detachment of microparticles. The nature of the ablation process in a femtosecond laser pulses regime differs from the ablation caused by the nanosecond and picoseconds laser pulses, which is presented in Figure 1.

Since the development of mode-locked lasers, ultrashort pulse durations became available, allowing measurements in the femtosecond range. The next significant advance in laser technology was the development of chirped pulse amplification

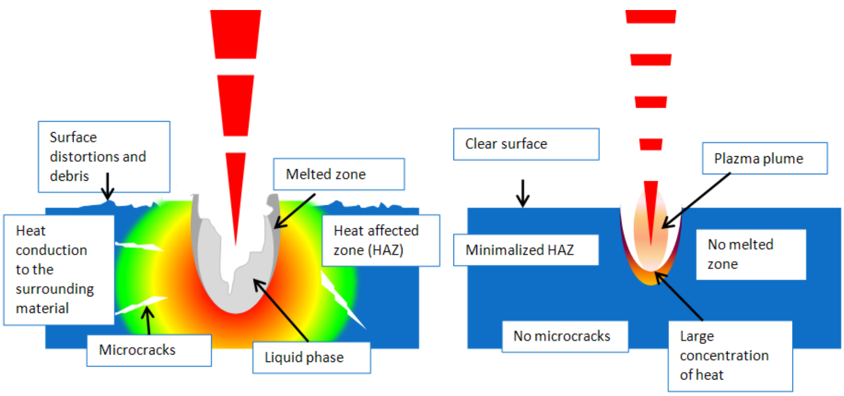

Figure 1. Long and ultrashort laser pulses interactions with matter.

(CPA) technique, which enabled pulse energies in the mJ range [2,3]. Thanks to this technique, Liu et al. were able to study the ablation dynamics with pulse width varying from 10 ns to 100 fs, and observed that the lowering of the ablation threshold was proportional to the shortening of the laser pulse [4]. However, the details of the physical mechanisms behind femtosecond laser ablation were still far from complete understanding.

A numerous groups studied the ablation processes analytically and numerically. Many models have been proposed to explain various aspects of the femtosecond ablation process including: ultrafast laser pulse absorption by solid targets, femtosecond heating, expansion, stress generation, defect capture and formation of periodic surface structures on surfaces [5-7].

The dynamics of the ablation process can be roughly divided into several stages: energy absorption, energy transfer to the lattice and subsequent material removal. The first step of the ablation process is deposition of energy into the material. The primary absorption mechanism involves excitation of electrons from the valance to the conduction band and free carrier absorption. The interband excitation can occur through nonlinear processes, such as multiphoton and avalanche ionization, with high enough laser intensity. Nonlinear absorption is very important in femtosecond interaction due to the high intensity of the incoming radiation [8]. During the laser-matter interaction all of the processes occur simultaneously and it is difficult to estimate the contribution of each one. Due to the complexity of the process, it is also difficult to calculate or measure the effective penetration depth of the radiation.

The energy transfer from electrons to the lattice occurs via carrier-phonon scattering on a timescale estimated from several hundred femtoseconds to a few picoseconds, depending on the material. Since the electrons and the lattice are not in equilibrium, this situation is often described by a two temperature model, where a distinction is made between the electron and the lattice temperature [9]. The energy transferred to the lattice leads to rapid thermal or nonthermal melting [10]. Since the timescale for mass transport is significantly longer than for nonthermal or even thermal melting, the melted material is left at near solid state densities and a high initial temperature. The subsequent processes of material removal have been described in terms of transient thermal processes. Following melting, the hydrodynamic expansion of the ablated material begins a few 100 ps after the initial excitation [11]. In spite of numerous investigations the fundamental mechanisms leading to the material removal are still rather poorly understood. Several different ablation mechanisms were identified in theoretical investigations including: spallation, explosive boiling, and vaporization [12-15].

Spallation occurs at a laser fluence just above the ablation threshold, and refers to ejection of material fragments induced by relaxation of the laser induced stresses. Higher fluence rates cause the transition to the phase explosion regime and the change in the dominant mechanism responsible for the material ejection.

The phase explosion id driven by the explosive release of the vapor. Phase explosion is believed to be the primary mechanism in femtosecond laser ablation, below the threshold of plasma formation [16]. At very high excitation fluences, the surface layer of the material can be completely atomized and the material is removed by vaporization.

The physics of ultrashort laser ablation of metals is essentially the same like in the case of dielectrics, semiconductors and polymers. The main difference is that in metals the electron density can be considered constant during the laser-matter interaction. In plastics, the electron density changes due to interband transitions and multiphoton and avalanche ionization followed by optical breakdown. The two temperature model is valid mainly for metals [17].

The entire ablation process occurs on time scales of several tens ns. Ablation experiments are usually performed with laser beams that have a near Gaussian spatial profile, therefore energy deposition varies across sample surface.

The ablation process mechanisms briefly described above depends, on the one hand, on the laser radiation parameters, such as pulse duration, wavelength, pulse energy, repetition rate or irradiation time, and on the other hand – material properties, i.e. absorption coefficient or thermal conductivity [9].

In laser – irradiated material sample, a various features, such as crater profiles, ablated volume, local changes in crystallography and chemistry, surface modifications can be related to various dynamical mechanisms and the ablation threshold and ablation rates can be readily obtained from the analysis of the final state of material.

Exploring the physical mechanisms during laser irradiation is crucial for the full understanding of the laser ablation phenomena. In the ultrashort pulse range, the most significant mechanisms are: liquid phase explosion due to the heterogenic and homogenic heating, due to the subsurface heating and the ablation plasma interactions with the material surface in so called Knudsen layer. Apart from the liquid phase ablation, the phenomena can also occur through direct sublimation. In that case, the most important ablation mechanisms are: spallation, fragmentation, charge separation due to avalanche and multiphoton ionization and coulomb explosion. The contribution of these particular mechanisms depends on the laser radiation parameters and material properties. Because of the complexity of the ablation process, a complete theory describing the laser-matter interactions in ultrashort pulse region has not been developed yet.

2 Methodology

The aim of this research is to investigate femtosecond interactions with matter under various processing parameters and on a wide group of materials. Therefore, a schematic research plan is presented in Figure 2, to enlist the parameters,

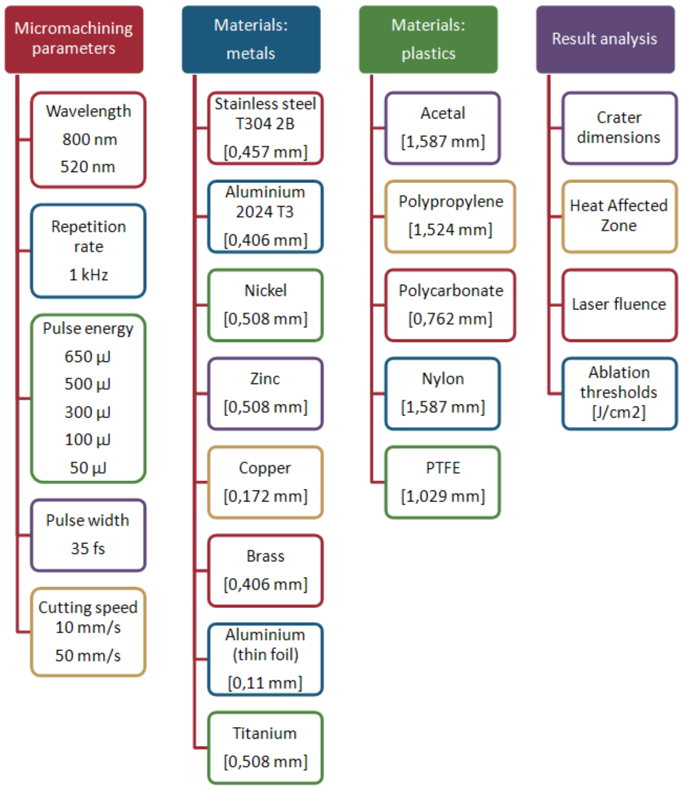

Figure 2. The scheme of the laser micromachining parametric study.

materials and significant post-processing analysis goals, taken under consideration in this study.

The experiments were conducted with two different setups dedicated to the two different values of laser wavelengths, shown in Figures 3-4. The source of the femtosecond laser pulses was a SpectraPhysics laser system, i.e. Ti:Sapphire ultrafast oscillator, ultrafast amplifier and a wavelength converter. The system offer 35 fs pulses of 1 kHz repetition rate, a tunable wavelength from 240 nm to 2600 nm and $>$ 6 mJ pulse energy.

In each setup, a 15 cm focusing lens together with several broadband mirrors, dedicated to the desired wavelength, was used to direct the laser beam to the machining area. A variable neutral density filter was applied directly at the laser output, to adjust the beam energy.

With the (A) experimental setup, a programmable, high precision Aerotech XY linear motor stage was used, to move the laser beam along the sample surface.

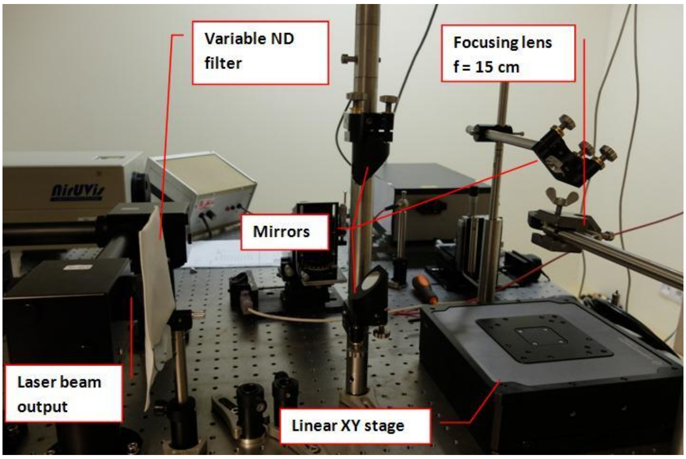

Figure 3. The experimental setup for 800 nm wavelength (A).

This variation of the (A) setup was applied to obtained high velocities in a machining process and is later referred to as "fast". In a "slow" variation of this setup, a linear XY stage with a significantly lower velocity was used. The later has been also used in the (B) setup. The anti-dust suction system was applied in both setups.

The samples were mounted directly on the linear stages, in the laser focus. The micromachining process was scribing a straight line, approximately 1–2 cm long, on the surface of the material. The process was applied to each of the sam-

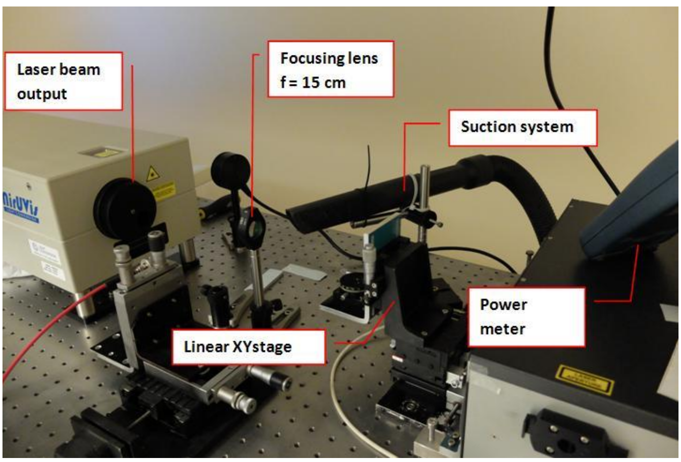

Figure 4. The experimental setup for 520 nm wavelength (B).

ples from "metals" group, using both of the setups (two different wavelength values). The materials from "plastic" groups were machined only using a "fast" variation, to prevent the significant heat damage of the samples, occurring when the velocity is too low.

In each setup variation, a parametric study with different laser pulse energy was conducted. The desired energy was obtained using the ND filter and varied from 50 μJ to 650 μJ. A power meter was used to confirm the energy value.

A Ti:S based femtosecond laser system offers very stable power levels in three different ranges of radiation (UV, VIS, IR), which makes it most adequate for various micromachining processes. Together with the optical focusing system and high precision positioning setup, it is suitable to achieve our research goals and have already proven a good quality of the results.

Evaluation of the experiment results is based mostly on the microscopic images. The stereoscopic metallographic microscope (up to 200× magnification) is used for crater dimensions, line width, HAZ range and debris measurements for most of the materials.

3 Results

The following results were obtained with a single femtosecond laser (detailed description can be found in the methodology chapter), which ensures a complexity of the research and guarantees constancy of the invariable parameters in each step.

As a reference, theoretical ablation thresholds for metals were calculated from eq. (1). Materials: thin metal foils and plastics, as listed in Table 1, were examined. The effects of the laser pulse parameters on ablation threshold, heat accumulation, ablation efficiency, cold and hot ablation mechanisms and the amount of liquid phase occurring during the laser irradiation are studied for each material. The specific material parameters, like absorption rate or heat conductivity are included as a significant variables.

$$F_{\mathrm{th}} = \frac{3}{8}(\varepsilon_{\mathrm{b}} + \varepsilon_{\mathrm{esc}})\frac{\lambda\eta_{\mathrm{a}}}{2\pi} \tag{1}$$

Table 1. Calculated ablation thresholds for materials used in the experiments

Wavelength	Stainless steel	Aluminium	Nickel	Zinc	Copper	Brass
800 nm	1.18 J/cm^2	1.06 J/cm^2	0.64 J/cm^2	0.63 J/cm^2	0.56 J/cm^2	0.56 J/cm^2
520 nm	0.77 J/cm^2	0.69 J/cm^2	0.42 J/cm^2	0.41 J/cm^2	0.36 J/cm^2	0.36 J/cm^2

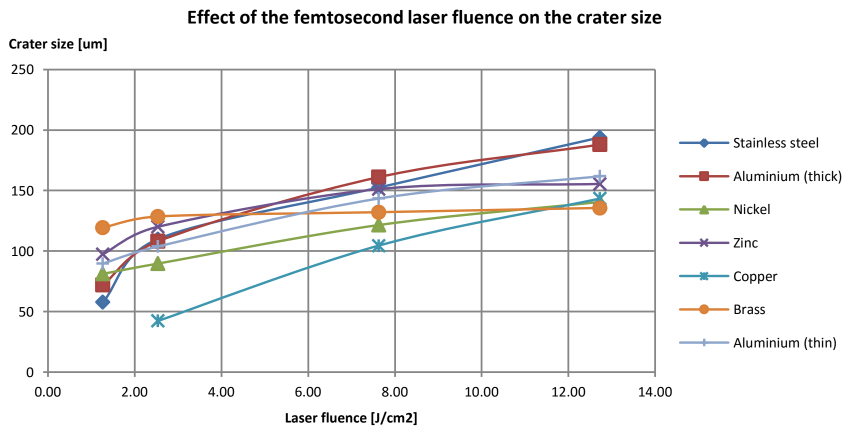

Figure 5. Laser micromachining of metals with various pulse energy.

A broad parametric study has been carried out on metals. Figure 5 represents the results of laser scribing process on the surface of metal samples with pulse energy varying from 50 μJ to 650 μJ. The study was conducted at 800 nm wavelength and 1 kHz pulse repetition rate. The results are represented as crater size dependency on laser fluence, as calculated form pulse energy per laser spot area. It is clear that the crater size increases nonlinearly with increasing power level. The shape of most of the characteristics is typical for femtosecond regime interactions, where an ablation threshold (more rapid rise of the crater size) is visible between the first two measurement points. From the presented samples, metals with lower ablation thresholds (nickel, zinc, copper) are forming a slightly different, more linear characteristics, usually typical for a picoseconds regime. The crater size is observed to be dependant not only on the material type, but also the sample thickness. The difference is visible on two aluminum samples of different thickness, with high fluencies. It can be concluded that this parameter has affected the results more than reflectivity and heat conductivity of the materials above a certain pulse energy. The laser-matter interaction time had to be very short compared to the heat conduction time from electrons to the lattice, which is frequent for the short-pulsed interactions, especially femtosecond. The theoretical calculated ablation threshold for these materials are similar, but usually lower than the experimental results.

A greater variety of the results was obtained with plastic materials (Figure 6). Most plastics showed ablation thresholds above 2 J/cm^2 and the crater size increasing more rapidly with the laser fluence. In the case of nylon and polycarbonate, higher laser fluencies damaged the material causing local melting and deformations and generating insignificant results. Very good machining quality and clean cuts were obtained with PTFE and polypropylene for each value of pulse energy.

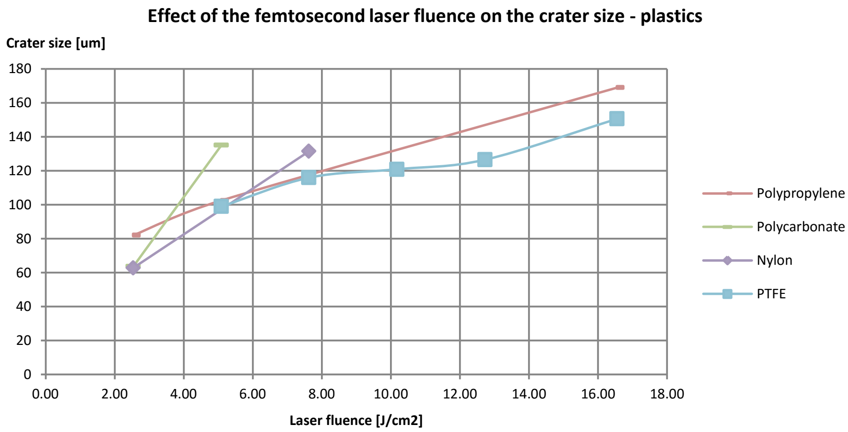

Figure 6. Laser micromachining of plastics with various pulse energy.

The effect of laser wavelength on crater size is unequivocal. As presented in Figure 7, the crater size is increasing with a lower wavelength. This tendency is true for each sample, yet independent of material group (metal or plastic) or the sample thickness. The slightest differences can be observed for PTFE and polycarbonate, which are partially transparent materials. The highest crater size obtained was for nylon and polypropylene in a VIS range, and for brass and zinc in an IR range. The smallest crater was obtained for copper in a IR range, which can be easily explained by the absorption coefficient of this material, which achieves its maximum value at about 500 nm a then decreases rapidly. The absorption rate is more constant for aluminum, steel and nickel, with a local

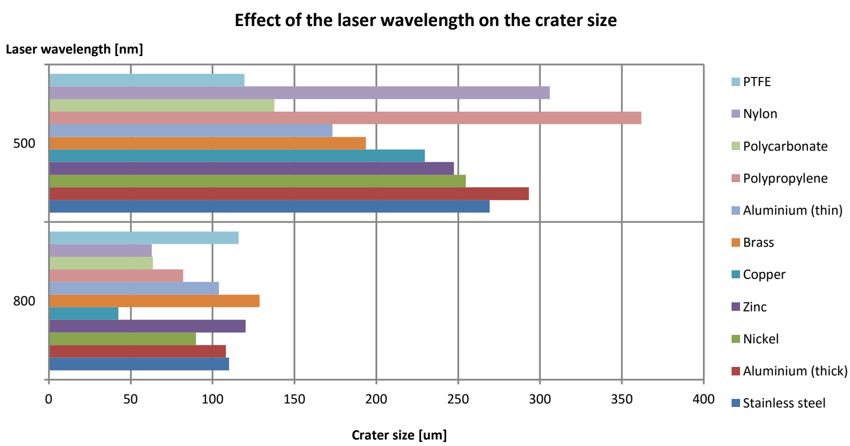

Figure 7. Laser micromachining of materials with two different wavelengths.

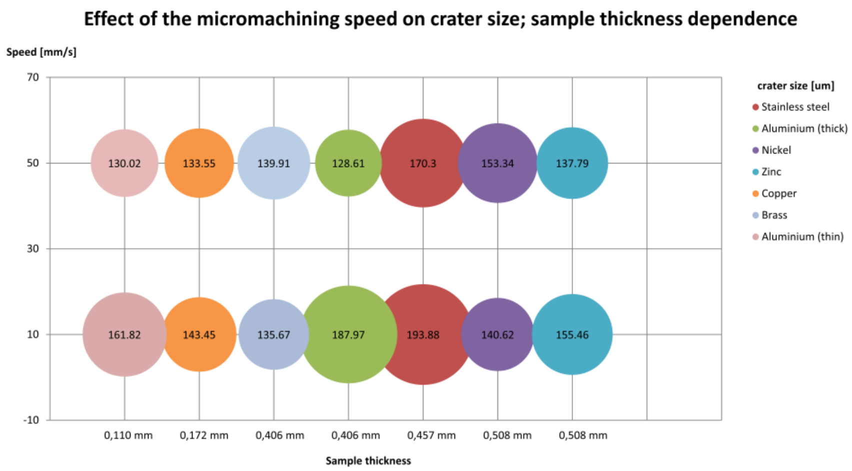

Figure 8. Laser micromachining of metals with two different machining velocities.

maximum at about 800 nm. The laser radiation from the IR range is therefore better absorbed for most metals, resulting in a higher quality of machining results. A fact, that could have disturbed some of the results, is that the laser fundamental beam is 520 nm, and after passing through a converter, the 800 nm beam may no longer have a gaussian profile.

The effect of the micromachining process on the crater size was measured with two different machining velocities, for which the samples were moved under the laser beam. Generally, the bigger craters were obtained with the lower velocity. With a laser beam moving slowly on the surface of the material sample, there were more time to distribute the heat inside the material. Therefore, more fine micromachining results were obtained with the higher velocity, i.e. with 50 mm/s.

In Figure 8, the size of the crater is represented by the size of the circle, and the samples are arrange by the thickness of the material. It can be observed, that with a lower machining speed, the crater size is more affected by the material type and sample thickness, and that more uniform results are achieved with 50 mm/s.

4 Conclusions

Femtosecond laser micromachining of several groups of materials was studied. Experiments have been conducted with various laser parameters and machining parameters. The results revealed very good efficiency and accuracy of the process, as well as a high quality of the machined structures.

It has been determined, that the size of the micromachining crater increases with the pulse energy, but decreases with the lengthening of the laser wavelength. The crater size increases more rapidly for plastics and depends also on sample thickness. The effect of the laser wavelength is highly dependable on the material type, due to the specific absorption rates.

The higher velocity of the machining process results in generally smaller crater size. The whole micromachining process is less dependent on the material type and sample thickness, when the speed increases.

During the laser micromachining process, the heat delivered into the material usually changes the area surrounding the target. Depending on the material used and machining type (cutting, drilling, engraving, dicing etc.), HAZ can cause local melting, deformation inside and debris on the surface of the material. The experiment results have shown that shortening the duration of the laser pulse to the range of femtoseconds significantly reduces HAZ, which translates into the high quality of the machined material.

Acknowledgements

The authors acknowledge the financial support of the EU FP7 Project INERA under the contract REGPOT 316309.

References

[1] N.P. Mahalik (2006) "Micromanufacturing and Nanotechnology", Springer.
[2] D. Strickland, G. Mourou (1985) *Opt. Commun.* **56** 219.
[3] G. Mourou (1997) *Appl. Phys. B* **65** 205.
[4] X. Liu, D. Du, G. Mourou (1997) *IEEE J. Quantum Electron.* **33** 1706.
[5] S.I. Anisimov, N.A. Inogamov, A.M. Oparin, B. Rethfeld, T. Yabe, M. Ogawa, V.E. Fortov (1999) *Appl. Phys. A* **69** 617.
[6] A. Peterlongo, A. Miotello, R. Kelly (1994)*Phys. Rev. E* **50** 4716.
[7] V.I. Emelyanov, D.V. Babak (2002) *Appl. Phys. A* **74** 797.
[8] K. Sokolowski-Tinten, D. von der Linde (2000) *Phys. Rev. B* **61** 2643.
[9] B.N. Chichkov, C. Momma, S. Nolte, F. van Alvensleben, A. Tunnerman (1996) *Appl. Phys. A* **63** 109.
[10] H.W.K. Tom. G.D. Aumiller, C.H. Brito-Cruz (1988) *Phys. Rev. Lett.* **60** 1438.
[11] K. Sokolowski-Tinten. L. Bialkowski. M. Doing. A, Cavalieri. D. von der Linde, A. Oparin, J. Mayer-ter-Vehn, S.I. Anisimov (1998) *Phys. Rev. Lett.* **81** 224.
[12] L.V. Zhigilei, B.J. Garrison (2000) *J. Appl. Phys.* **88** 1281.
[13] D. Perez, L.J. Lewis (2002) *Phys. Rev. Lett.* **89** 255504.
[14] C. Shafer, H.M. Urbassek, L.V. Zhigilei (2002) *Phys. Rev. B* **66** 115404.
[15] D.S. Ivanov, L.V. Zhigilei (2003) *Phys. Rev. Lett.* **91** 105701.
[16] D. Perez, L.J. Lewis (2003)*Phys. Rev. B* **67** 184102.
[17] M.E. Fermann, A. Galvanauskas, G. Sucha (2005) "Ultrafast Lasers: Technology and Applications", Marcel Dekker, Inc.